Supplemental Information

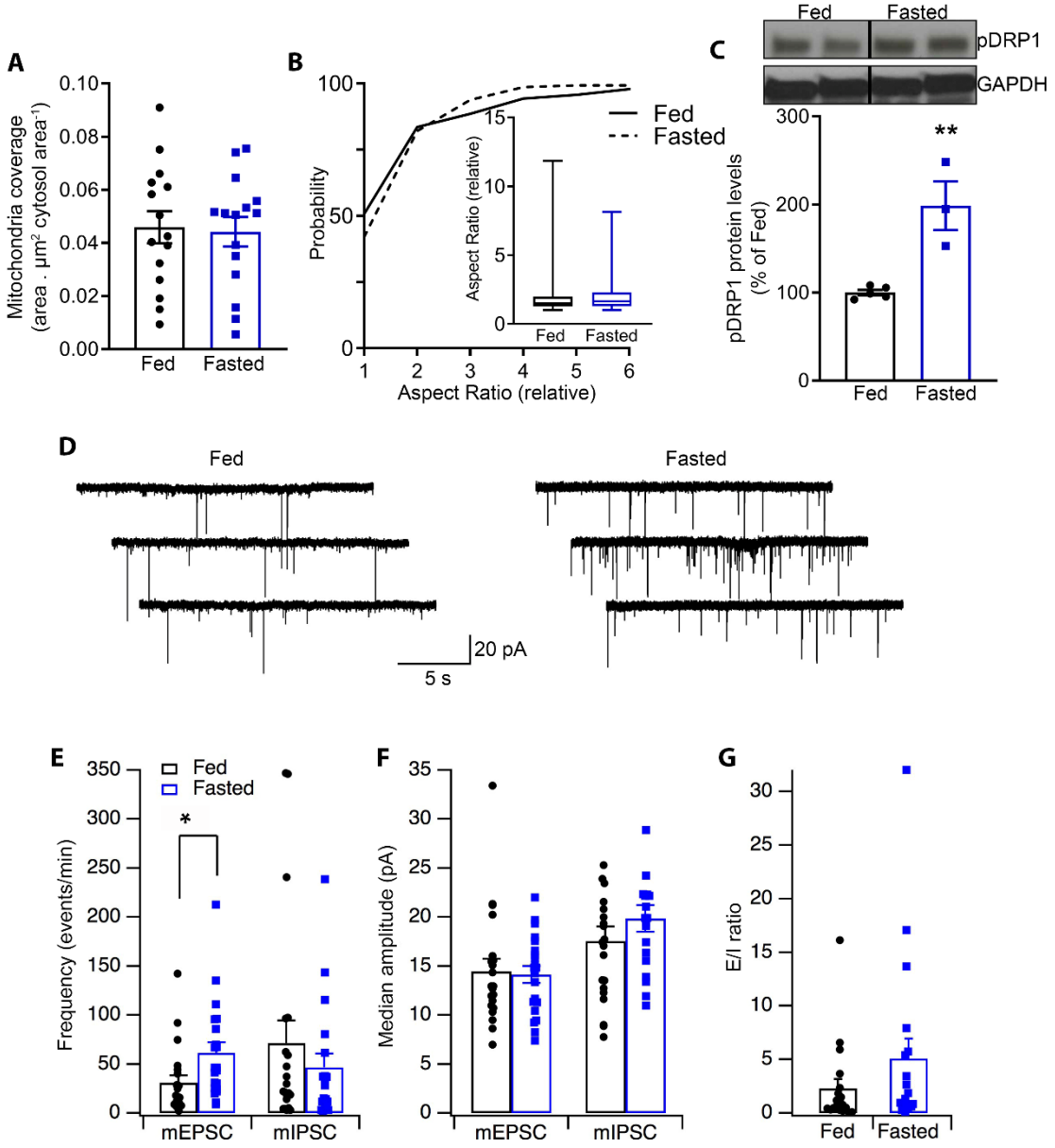

Suppl. Figure 1. A) Mitochondria coverage in Arc astrocytes of fed and fasted mice (n = 15 cells per group from 4-5 mice). B) Cumulative distribution and mean of mitochondria aspect ratio of fed and fasted mice (n = 140/145 mitochondria from 4-5 mice). C) pDRP1 levels (representative western blot images and quantification) from MBH of fed and fasted mice (n = 5/3 mice) (lanes were run on the same gel but were noncontiguous). D) Representative traces of mEPSC in NPY-GFP neurons of fed (left panel) and fasted (right state) mice. Quantification of E) frequency and F) amplitude of mEPSC and mIPSC in NPY-GFP neurons of fed and fasted mice (n =21,21,21,19). G) Ratio mEPSC/mIPSC in NPY-GFP neurons on fed and fasted mice. Data are presented as mean ± SEM. *p ≤ 0.05, **p≤ 0.01 and ***p≤ 0.001 as determined by two-tailed t-test or Kolmogorov-Smirnov test for analyses of cumulative distribution.

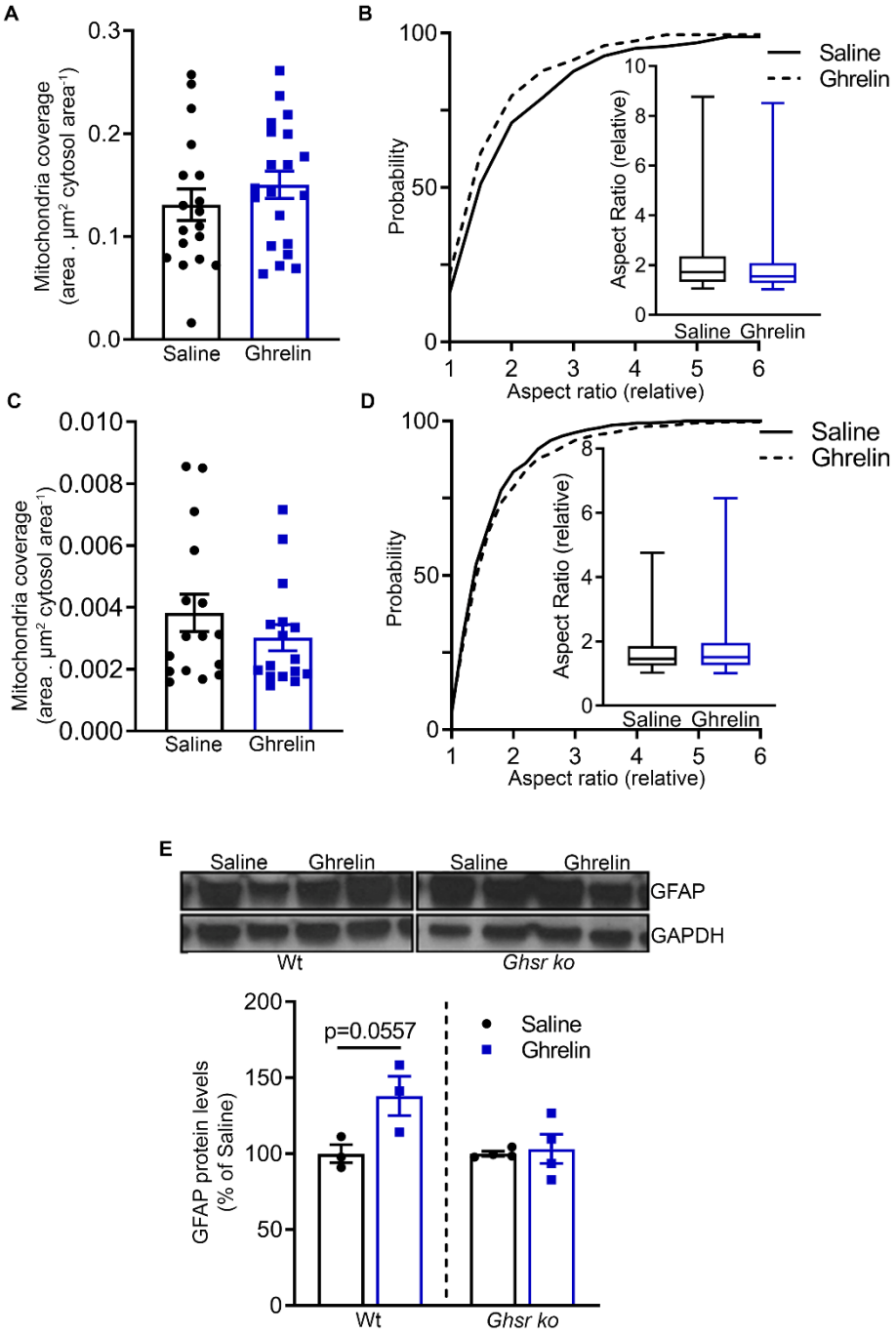

Suppl. Figure 2. A) Mitochondria coverage in Arc astrocytes of saline- and ghrelin-treated mice (n =18/20 18 cells). B) Cumulative distribution and mean of mitochondria aspect ratio in Arc astrocytes of saline- and ghrelin-treated mice (n = 164/199 mitochondria). C) Mitochondria coverage in NPY cells of saline- and ghrelin-treated mice (n = 16/17 cells). D) Cumulative distribution and mean of mitochondria aspect ratio in NPY cells of saline- and ghrelin-treated mice (n = 463/370 mitochondria). E) GFAP levels (representative western blot images and quantification) from MBH of Wt and *Ghsr ko* mice after saline or ghrelin administration (n=3/3/4/4 mice) (lanes were run on the same gel but were noncontiguous). Data are presented as mean ± SEM. *p ≤ 0.05, **p≤ 0.01 and ***p≤ 0.001 as determined by two-tailed t-test or Kolmogorov-Smirnov test for analyses of cumulative distribution.

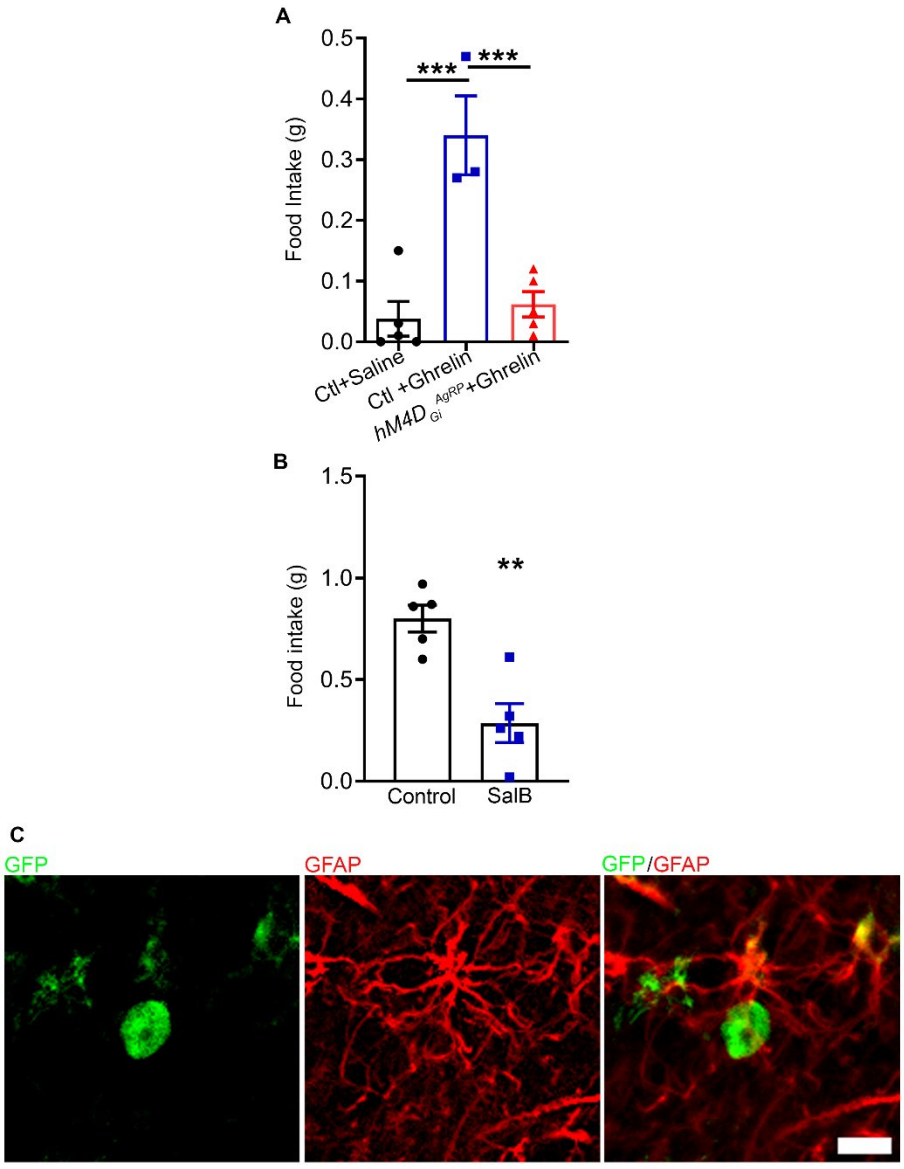

Suppl. Figure 3. A) Food intake (2h) after the Saline or ip. ghrelin administration of control and hM4D$_{Gi}^{AgRP}$ mice. Mice were treated with either CNO or Vehicle 15 minutes before the peripheral saline or ghrelin treatment (n = 3/5). B) Food intake (1h) of AgRP-Cre+ AAV-KORD-mCitrine after saline or SalB treatment (n = 5/5). C) Representative images from AgRP-Cre +AAV-KORD-mCitrine, Green depicts an AgRP neurons infected by the AAV. Red depicts an astrocyte labelled with GFAP staining. No astrocytes were infected by AAV-KORD-mCitrine. Scale Bars,10 µm. Data are presented as mean ± SEM. *p ≤ 0.05, **p≤ 0.01 and ***p≤ 0.001 as determined by one-way ANOVA (A) or two-tailed t-test (B).

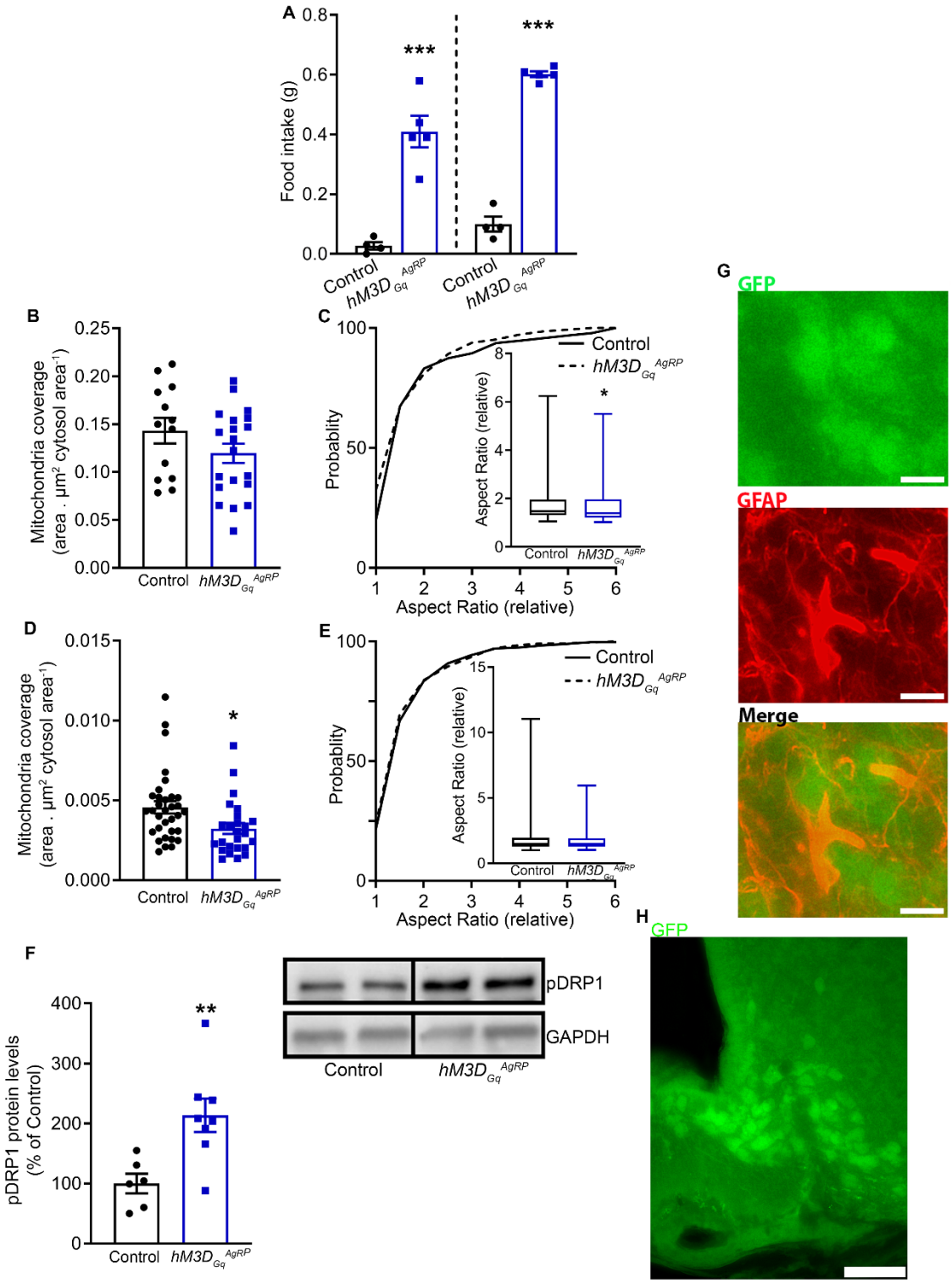

Suppl. Figure 4. A) Food intake (1h and 2h) after CNO administration of control and hM3D$_{Gq}^{AgRP}$ mice (n = 4/5). B) Mitochondria coverage in Arc astrocytes of control and *hM3D$_{Gq}^{AgRP}$* mice (n = 13/20 cells, 3-4 mice). C) Cumulative distribution and mean of mitochondria aspect ratio in Arc astrocytes of control and hM3D$_{Gq}^{AgRP}$ mice (n = 95/147 mitochondria). D) Mitochondria coverage in AgRP/NPY neurons of control and hM3D$_{Gq}^{AgRP}$ mice (n =33/ 25 cells, 5-6 mice). E) Cumulative distribution and mean of mitochondria aspect ratio in AgRP/NPY neurons from control and hM3D$_{Gq}^{AgRP}$ mice (n = 709/665 mitochondria). F) Representative blots and protein expression levels of pDRP1 in the MBH of control and hM3D$_{Gq}^{AgRP}$ mice (n=6/8 mice) (lanes were run on the same gel but were noncontiguous). G) Representative images from hypothalamus of hM3D$_{Gq}^{AgRP}$ mice (green) stained with GFAP antibody (red). Co-localization was not found. Scale Bars, 10 µm. H) Representative images from hypothalamus of hM3D$_{Gq}^{AgRP}$ mice (green). Signal was limited exclusively to the Arc. Scale bar, 50 µm. Data are presented as mean ± SEM. *p ≤ 0.05, **p≤ 0.01 and ***p≤ 0.001 as determined by two-tailed t-test or Kolmogorov-Smirnov test for analyses of cumulative distribution.

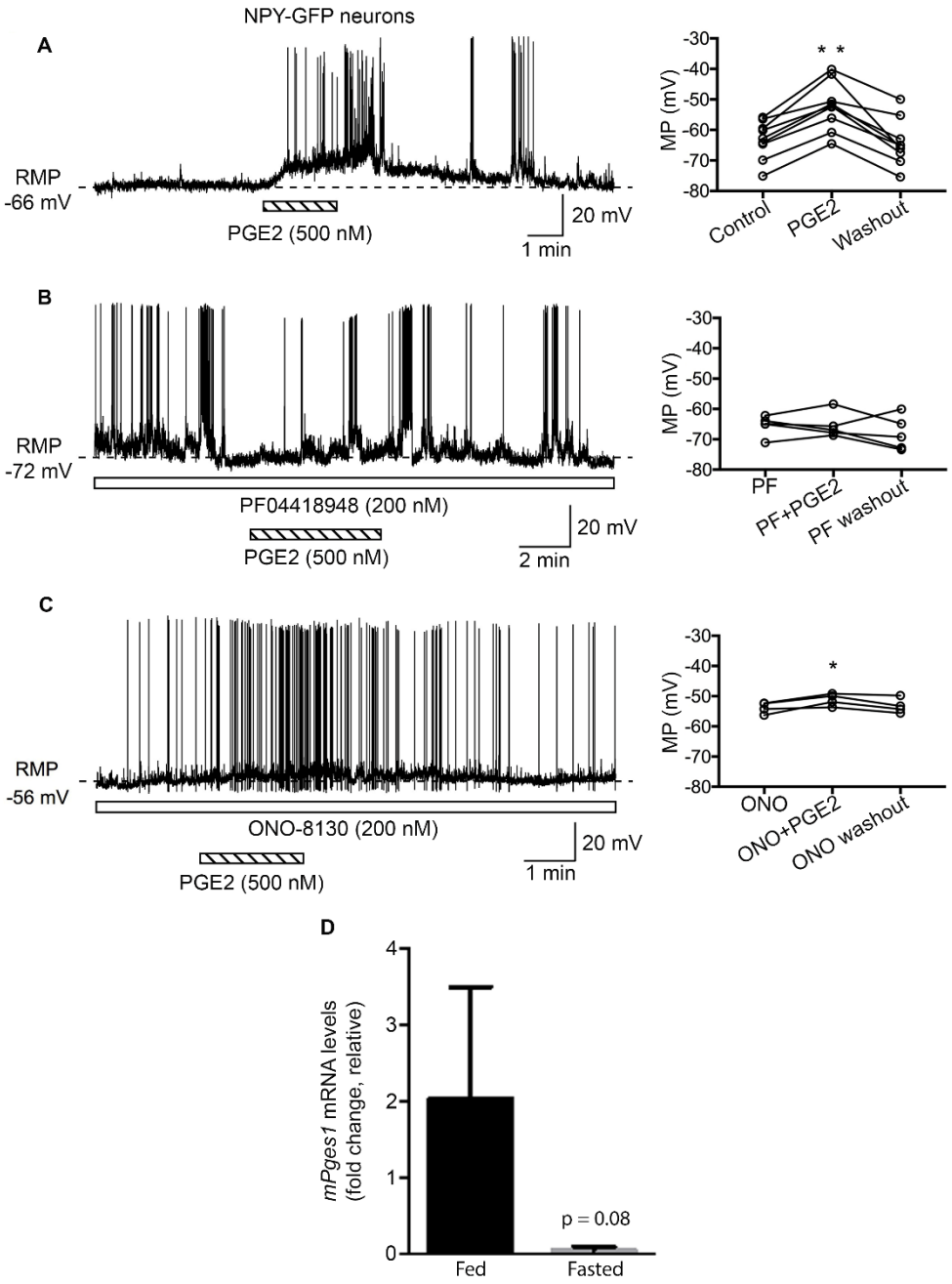

Suppl. Figure 5. Left panel of A) Representative trace of an NPY-GFP neuron before and during the application of PGE2. Right panel of a) Membrane potential of arcuate nucleus NPY-GFP neurons (n=9) before (Control) and during the application of PGE2 and after washout. Left panel of B) Representative trace of an NPY-GFP neuron before and during the application of PGE2 and after washout while exposed to the EP2 receptor inhibitor, PF0441894 (PF). Right panel of B) Membrane potential of arcuate nucleus NPY-GFP neurons (n=4) before and during the application of PGE2and after washout while exposed to the EP2 receptor inhibitor (PF). Left panel of C) Representative trace of an NPY-GFP neuron before and during the application of PGE2 and after washout while exposed to the EP1 receptor inhibitor, ONO-8130 (ONO). Right panel of C) Membrane potential of arcuate nucleus NPY-GFP neurons (n=4) before and during the application of PGE2 and after washout while exposed to ONO. D) *mPges1* mRNA levels from hypothalamic astrocytes of fed and fasted mice. Data are presented as mean ± SEM * $p \leq 0.05$, ** $p \leq 0.01$ as determined by one-way ANOVA (A, B and C) or two-tailed t-test (D).